Research Square

Preprints are preliminary reports that have not undergone peer review.
They should not be considered conclusive, used to inform clinical practice,
or referenced by the media as validated information.

Functional Activity and Cerebral Perfusion Alterations in Meige Syndrome: A Resting-State Functional Magnetic Resonance Imaging and Arterial Spin Labeling Study

Jia Wang
China-Japan Friendship Hospital
Yian Gao
China-Japan Friendship Hospital
Manxi Xu
China-Japan Friendship Hospital
Peiling Ou
China-Japan Friendship Hospital
Haoyu Yang
China-Japan Friendship Hospital
Wulong Liu
China-Japan Friendship Hospital
Zhen Yuan
University of Macau
Shilong Sun
China-Japan Friendship Hospital
Yuli Wang
China-Japan Friendship Hospital
Hongwei Yu
China-Japan Friendship Hospital
Tongxi Liu
China-Japan Friendship Hospital
Guolin Ma
maguolin1007@qq.com

China-Japan Friendship Hospital

Research Article

Keywords: Meige syndrome, functional magnetic resonance imaging, cerebral blood flow, amplitude of low-frequency fluctuation, regional homogeneity

Posted Date: June 22nd, 2026

DOI: https://doi.org/10.21203/rs.3.rs-9593437/v1

License: This work is licensed under a Creative Commons Attribution 4.0 International License.
Read Full License

Additional Declarations: No competing interests reported.

Functional Activity and Cerebral Perfusion Alterations in Meige Syndrome: A Resting-State Functional Magnetic Resonance Imaging and Arterial Spin Labeling Study

Abstract

Purpose: Meige syndrome is an adult-onset segmental dystonia characterized by blepharospasm and oromandibular dystonia, but its alterations in spontaneous brain activity and cerebral perfusion remain unclear. This study aimed to characterize abnormalities in spontaneous neural activity and cerebral perfusion in Meige syndrome using resting-state functional magnetic resonance imaging (rs-fMRI) and arterial spin labeling (ASL), and to assess their clinical relevance.

Methods: In this study, 28 patients with Meige syndrome and 32 matched healthy controls underwent rs-fMRI and ASL. Group differences in amplitude of low-frequency fluctuation (ALFF), regional homogeneity (ReHo), and normalized cerebral blood flow (CBF) were assessed. Correlation analyses examined associations between imaging metrics and clinical measures, and receiver operating characteristic analysis evaluated discriminatory performance.

Results: Relative to controls, patients showed reduced ALFF in the left anteromedial cingulate gyrus and bilateral medial superior frontal gyri, reduced ReHo in the bilateral medial superior frontal gyri, and increased normalized CBF in several primary motor cortex subregions. ALFF in the right medial superior frontal gyrus was inversely correlated with Blepharospasm Disability Index scores, whereas ReHo in the same region was inversely correlated with Self-Rating Depression Scale scores. Normalized CBF in the right precentral gyrus differentiated patients from controls with an area under the curve of 0.861.

Conclusion: Meige syndrome is associated with convergent abnormalities in medial frontal activity and primary motor cortex perfusion. These findings support the involvement of frontal-motor network dysfunction in its pathophysiology and suggest that regional perfusion metrics may serve as candidate imaging biomarkers.

Keywords: Meige syndrome; functional magnetic resonance imaging; cerebral blood flow; amplitude of low-frequency fluctuation; regional homogeneity.

1. Introduction

Meige syndrome, also referred to as blepharospasm-oromandibular dystonia syndrome, is a rare form of segmental dystonia [1]. It typically has an adult onset, with most patients developing symptoms between 30 and 70 years of age, and is more common in women, with a female-to-male ratio of approximately 2–3:1 [2]. Although its diagnosis still relies largely on clinical symptom recognition and physician experience, objective biological markers remain lacking. Elucidating the neural mechanisms of Meige syndrome is therefore important for improving pathophysiological understanding and facilitating the identification of objective imaging biomarkers.

Emerging evidence suggests that Meige syndrome is not simply attributable to dysfunction in a single focal brain region, but rather may involve distributed brain network abnormalities related to

impaired central inhibition, disordered sensorimotor integration, and maladaptive neuroplasticity [3,4]. Recent connectomic studies have further shown that Meige syndrome is associated with whole-brain topological alterations, including reduced nodal efficiency in specific functional networks and decoupling of structural and functional connectivity [5,6]. However, abnormalities at the whole-brain network level may be partly rooted in alterations in local spontaneous neural activity and regional cerebral blood perfusion.

Although conventional structural MRI often fails to reveal definite abnormalities in patients with Meige syndrome, advanced MRI techniques can provide important insights into functional and perfusion-related alterations. Previous resting-state functional MRI (fMRI) studies have shown abnormal functional connectivity in the basal ganglia, cerebellum, sensorimotor cortex, and visual-related regions in patients with Meige syndrome [7]. Arterial spin labeling (ASL), a noninvasive perfusion MRI technique, enables quantitative assessment of cerebral blood flow (CBF), and prior studies have reported increased CBF in the middle frontal gyrus and bilateral precentral gyri in these patients [8]. Together, these findings suggest that Meige syndrome may be associated with abnormalities in both brain functional activity and cerebral perfusion, although the available evidence remains limited.

Amplitude of low-frequency fluctuation (ALFF) and regional homogeneity (ReHo) are commonly used resting-state fMRI metrics that reflect the intensity of spontaneous low-frequency oscillations and the temporal synchronization of local neural activity, respectively [9,10]. However, studies using ALFF and ReHo to investigate local spontaneous brain functional abnormalities in Meige syndrome remain scarce, and ASL-based studies of cerebral perfusion abnormalities are also limited.

Therefore, in the present study, we combined resting-state fMRI and ASL to investigate alterations in local brain functional activity and cerebral perfusion in patients with Meige syndrome. We further analyzed the associations between these imaging findings and clinical symptom severity, with the aim of providing imaging evidence to help elucidate the neural mechanisms underlying the disease.

2. Materials and Methods

2.1 Clinical Data

This was a cross-sectional study. A total of 30 patients with Meige syndrome who attended a tertiary medical center between September 2020 and January 2022, as well as 32 healthy controls recruited from the local community during the same period, were retrospectively enrolled. Demographic characteristics, multidimensional neurological scale data, resting-state functional magnetic resonance imaging (rs-fMRI) data, and arterial spin labeling (ASL) data were collected for all participants. After imaging quality control, 2 patients with Meige syndrome were excluded because of excessive head motion, leaving 28 patients with Meige syndrome and 32 healthy controls for the final rs-fMRI and ASL analyses.

The inclusion criteria for patients with Meige syndrome were as follows: (a) all patients were diagnosed with primary Meige syndrome by an experienced senior neurosurgeon according to

established clinical criteria [11]; (b) no abnormal findings were detected on routine brain MRI; (c) no treatment had been administered within 3 months prior to enrollment; and (d) right-handedness. The exclusion criteria were as follows: (a) organic brain disease; (b) neuropsychiatric disorders; (c) other forms of dystonia besides Meige syndrome; (d) a history of severe pulmonary, cardiac, hepatic, or renal disease; and (e) contraindications to MRI examination. This study was approved by the institutional ethics committee. Written informed consent was obtained from all participants.

Multidimensional neurological assessments mainly included the Burke-Fahn-Marsden Dystonia Rating Scale-Movement subscale (BFMDRS-M) and the Blepharospasm Disability Index (BSDI) [12] to evaluate disease severity. In addition, all patients with Meige syndrome were assessed using the Self-Rating Depression Scale (SDS) and the Self-Rating Anxiety Scale (SAS) to evaluate the severity of depressive and anxiety symptoms.

2.2 MRI Acquisition Parameters

MRI examinations were performed using a 3.0-T scanner (Discovery MR750, GE Healthcare, Milwaukee, WI, USA) equipped with a standard 8-channel head coil at the participating institution. Foam padding and earplugs were used to minimize head motion and scanner noise. During image acquisition, all participants were instructed to remain still in the supine position with their eyes closed, while staying awake, relaxed, and not engaging in specific mental activity.

The imaging protocol included routine MRI sequences, including T2-weighted imaging, T2 fluid-attenuated inversion recovery, and diffusion-weighted imaging, to exclude intracranial lesions and ensure strict adherence to the inclusion and exclusion criteria, as well as sagittal three-dimensional T1-weighted structural imaging, rs-fMRI, and ASL sequences.

The scan parameters were as follows. For the 3D T1-weighted sequence: repetition time (TR) = 8.2 ms, echo time (TE) = 3.2 ms, field of view (FOV) = 240 × 240 mm, matrix = 256 × 256, slice thickness = 1.2 mm, number of excitations (NEX) = 1, number of slices = 156, and acquisition time = 4 min 10 s. For rs-fMRI: TR = 2000 ms, TE = 30 ms, flip angle = 90°, slice thickness = 3.5 mm, NEX = 1, number of slices = 34, FOV = 224 × 224 mm, matrix = 64 × 64, and acquisition time = 8 min. For ASL: TR = 4817 ms, TE = 14.6 ms, post-labeling delay (PLD) = 1525 ms, slice thickness = 4 mm, number of slices = 36, FOV = 240 × 240 mm, matrix = 128 × 128, and acquisition time = 6 min 54 s.

2.3 Image Analysis

2.3.1 Resting-State fMRI Analysis

Resting-state fMRI data were converted from DICOM to NIfTI format using dcm2nii (MRIcron). Image preprocessing was performed using DPARSF [13,14] on the MATLAB 2013b platform. The preprocessing steps included removal of the first 10 time points, slice timing correction, head motion correction, exclusion of subjects with head displacement > 2 mm or rotation > 2°, spatial normalization, spatial smoothing with a 4-mm full-width at half-maximum Gaussian kernel, and linear detrending.

ALFF and ReHo were calculated using DPARSF. After band-pass filtering (0.01-0.08 Hz) and Fourier transformation, voxel-wise ALFF values, standardized ALFF values (zALFF), and statistical parametric maps were obtained. ReHo values were calculated as Kendall's coefficient of concordance by measuring the temporal consistency of each voxel with its 26 neighboring voxels.

2.3.2 ASL Data Processing and Analysis

CBF maps were generated from the ASL data using GE FuncTool perfusion software (GE Healthcare). In brief, CBF maps were derived by subtracting the labeled images from the control images, and quantitative CBF was calculated from the ASL difference images and proton density-weighted reference images using a single-compartment model [15,16].

Individual CBF maps in native space were directly registered to the perfusion template in SPM8 and then spatially normalized to Montreal Neurological Institute (MNI) space. Subsequently, the Brainnetome atlas [17] was overlaid to extract the mean CBF values of the whole brain and the precentral gyrus subregions. Previous studies have shown that the primary motor cortex (precentral gyrus) is a key cortical region involved in motor function in Meige syndrome. In addition, the present voxel-wise whole-brain comparison of CBF revealed significant between-group differences in the precentral gyrus. Therefore, according to the Brainnetome atlas, the bilateral precentral gyri were subdivided into six subregions as regions of interest (ROIs), and the normalized CBF value for each subregion was calculated. The ROIs used in this study are shown in Table 1 and Fig. 1.

Table 1 Parcellation and basic information of the six ROI subregions within the bilateral precentral gyri

ROIs	Anatomical descriptions	Left hemisphere MNI coordinates (X,Y,Z)	Right hemisphere MNI coordinates (X, Y, Z)
PrG_L(R)_6_1	Area 4 (head and face region)	(-49, -8, 39)	(55, -2, 33)
PrG_L(R)_6_2	Caudal dorsolateral area 6	(-32, -9, 58)	(33, -7, 57)
PrG_L(R)_6_3	Area 4 (upper limb region)	(-26, -25, 63)	(34, -19, 59)
PrG_L(R)_6_4	Area 4 (trunk region)	(-13, -20, 73)	(15, -22, 71)
PrG_L(R)_6_5	Area 4 (tongue and larynx region)	(-52, 0, 8)	(54, 4, 9)
PrG_L(R)_6_6	Caudal ventrolateral area 6	(-49, 5, 30)	(51, 7, 30)

PrG：precentral gyrus; MNI, Montreal Neurological Institute.

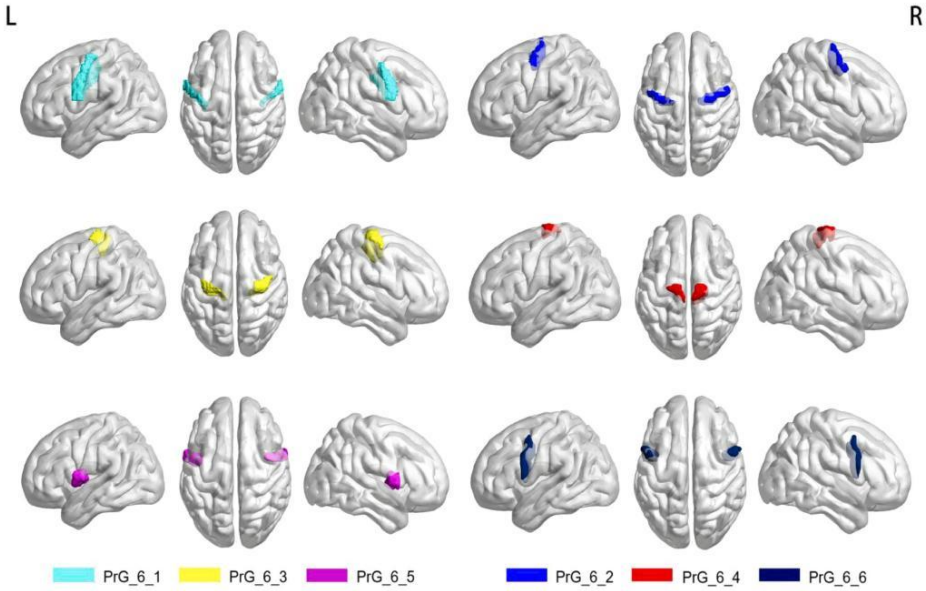


Fig. 1 Anatomical distribution of the six subregions within the bilateral precentral gyri.
The subregions PrG_6_1 through PrG_6_6 are shown in light blue, dark blue, yellow, red, purple, and navy, respectively.
Abbreviations: PrG = precentral gyrus; L = left; R = right.

2.4 Statistical Analysis

Statistical analyses of clinical variables and ROI-level data were performed using SPSS 26.0. Normality was assessed using the Shapiro–Wilk test. Normally distributed data are presented as mean ± standard deviation, whereas non-normally distributed data are presented as median with interquartile range. Categorical variables were compared using the chi-square test, and between-group comparisons were performed using the independent-samples t test or the nonparametric test for two independent samples, as appropriate. Whole-brain voxel-wise comparisons of ALFF, ReHo, and normalized CBF were performed using the independent-samples t test. Multiple-comparison correction was performed using FWE, GRF, and FDR methods: ALFF and normalized CBF were corrected using FWE correction ($P < 0.05$), ReHo was corrected using Gaussian random field (GRF) correction (voxel-level $P < 0.001$, cluster-level $P < 0.05$, two-tailed), and ROI-level normalized CBF was corrected using FDR correction ($P < 0.05$). Correlation analyses were performed using Pearson or Spearman correlation analysis, as appropriate; receiver operating characteristic (ROC) analysis was further performed for statistically significant parameters. A P value < 0.05 was considered statistically significant.

3. Results

3.1 Demographic and Clinical Characteristics

A total of 28 patients with Meige syndrome and 32 healthy controls were ultimately included in this study. There were no significant between-group differences in age, sex, body weight, or years of education (all $P > 0.05$) (Table 2).

Table 2 Demographic and clinical characteristics of patients with Meige syndrome and healthy controls

Clinical Characteristics	Meige Group (n=28)	Healthy Control Group (n=32)	P value
Age (years)	59.04±8.45	61.13±7.24	0.307
Gender (Male/Female)	7/21	10/22	0.592
Weight (kg)	65.38±12.12	63.41±7.65	0.463
Education (years)	9.00 (6.00-12.00)	9.00 (9.00-12.00)	0.283
Disease Duration (months)	24.00 (12.00-57.00)	–	–
BFMDRS-M	6.75 (5.50-9.00)	–	–
Average BSDI	2.14±0.94	–	–
Total BSDI	12.57±5.67	–	–
SDS	40.50 (36.00-45.00)	–	–
SAS	41.25±9.13	–	–

BFMDRS-M, Burke–Fahn–Marsden Dystonia Rating Scale-Movement; BSDI, Blepharospasm Disability Index; SDS, Self-Rating Depression Scale; SAS, Self-Rating Anxiety Scale. Normally distributed data are presented as mean ± standard deviation, whereas non-normally distributed data are presented as median (interquartile range).

3.2 Between-Group Comparisons of ALFF and ReHo Values in Patients With Meige Syndrome and Healthy Controls

Compared with healthy controls, patients with Meige syndrome showed significantly decreased ALFF values in the left anteromedial cingulate gyrus and bilateral medial superior frontal gyri ($P < 0.05$, FWE corrected). In addition, patients with Meige syndrome showed significantly decreased ReHo values in the bilateral medial superior frontal gyri (voxel-level $P < 0.001$, cluster-level $P < 0.05$, two-tailed, GRF corrected) (Table 3; Fig. 2).

Table 3 Results of statistically significant differences in ALFF and ReHo values between groups

item	group	MNI region	Peak MNI coordinate			Number of voxels	T value
			x	y	z		
ALFF	Meige < HC	Left anteromedial cingulate gyrus	-9	-9	33	103	-5.0154
		Left medial superior frontal gyrus	-9	54	18	42	-5.6040
		Right medial superior frontal gyrus	9	57	21	8	-4.3096
ReHo	Meige < HC	Left medial superior frontal gyrus	-15	39	24	98	-4.8921
		Right medial superior frontal gyrus	15	51	15	66	-4.6824

HC, healthy control； MNI, Montreal Neurological Institute

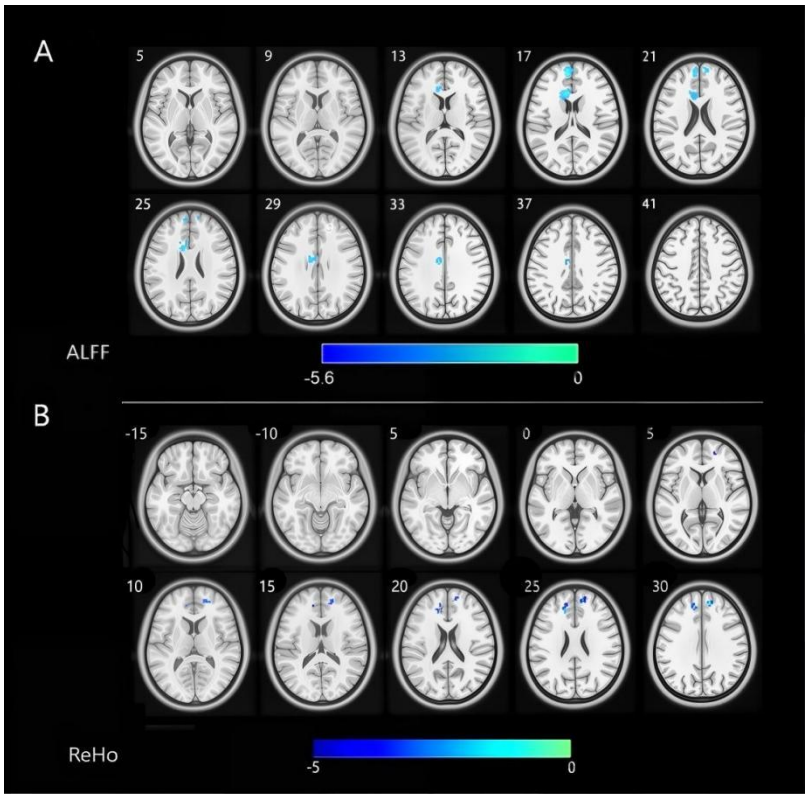


Fig. 2 Differences in ALFF and ReHo values between patients with Meige syndrome and healthy controls.

(A) Patients with Meige syndrome showed reduced ALFF values in the left anterior cingulate cortex and bilateral medial superior frontal gyri. Results are shown on axial slices; blue clusters indicate statistically significant regions ($P < .05$, family-wise error corrected). The color bar represents T values.

(B) Patients with Meige syndrome showed reduced ReHo values in the bilateral medial superior frontal gyri. Results are shown on axial slices; blue clusters indicate statistically significant regions (voxel-level $P < .001$; cluster-level $P < .05$; two-tailed; Gaussian random field corrected). The color bar

represents *T* values.
Abbreviations: ALFF = amplitude of low-frequency fluctuation; ReHo = regional homogeneity.

3.3 Between-Group Comparisons of CBF Values at the Voxel-Wise and ROI Levels

We found significant differences in normalized CBF values between patients with Meige syndrome and healthy controls. Voxel-wise analysis revealed one statistically significant cluster in the right precentral gyrus (cluster size: 15 voxels; peak MNI coordinates: 26, −18, 71; T = 5.92; FWE-corrected P = 0.017), indicating that normalized CBF in the right precentral gyrus was significantly higher in patients with Meige syndrome than in healthy controls (Fig. 3). Further ROI-level analysis showed that normalized CBF values also differed significantly between the Meige syndrome and healthy control groups in several precentral gyrus subregions. Compared with healthy controls, patients with Meige syndrome exhibited significantly increased normalized CBF values in PrG_L_6_2, PrG_R_6_2, PrG_L_6_3, and PrG_R_6_4 (all P < 0.05, FDR-corrected; see Table 4 and Fig. 4).

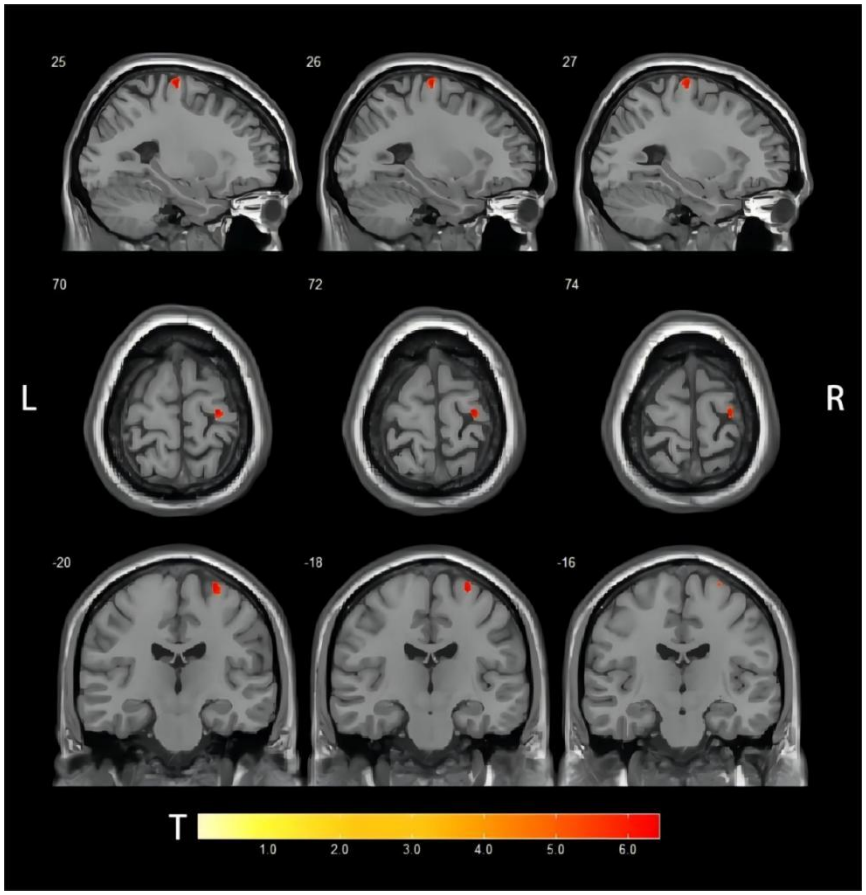


Fig. 3 Increased voxel-wise normalized CBF in patients with Meige syndrome compared with healthy controls.
Patients with Meige syndrome showed higher voxel-wise normalized CBF values in the right precentral gyrus. Results are shown on sagittal, axial, and coronal slices; red clusters indicate statistically significant regions ($P < .05$, family-wise error corrected). The color bar represents *T* values.
Abbreviations: CBF = cerebral blood flow.

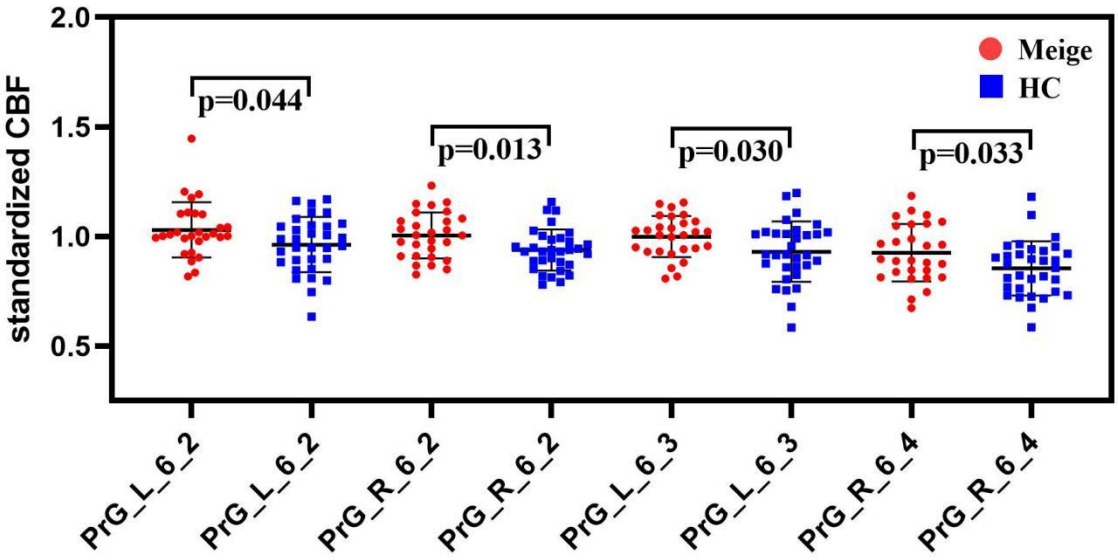


Fig. 4 Comparison of normalized CBF values in selected precentral gyrus regions of interest between patients with Meige syndrome and healthy controls.

Normalized CBF values in PrG_L_6_2, PrG_R_6_2, PrG_L_6_3, and PrG_R_6_4 were significantly higher in patients with Meige syndrome than in healthy controls ($P < .05$, false discovery rate corrected).

Abbreviations: CBF = cerebral blood flow; PrG = precentral gyrus; L = left; R = right.

Table 4 Group differences in normalized CBF values within the ROI subregions

ROIs	**normalized CBF**		T value	P value
	Meige group	HC group		
PrG_L_6_1	1.120±0.119	1.079±0.121	1.327	0.190
PrG_R_6_1	1.063±0.160	1.068±0.123	-0.143	0.887
PrG_L_6_2	1.030±0.126	0.963±0.126	2.060	**0.044***
PrG_R_6_2	1.005±0.105	0.938±0.095	2.572	**0.013***
PrG_L_6_3	0.999±0.094	0.931±0.137	2.221	**0.030***
PrG_R_6_3	1.002±0.121	0.954±0.137	1.433	0.157
PrG_L_6_4	0.885±0.161	0.817±0.118	1.883	0.065

PrG_R_6_4	0.926±0.131	0.854±0.124	2.178	**0.033***
PrG_L_6_5	1.157±0.093	1.140±0.167	0.487	0.629
PrG_R_6_5	1.096±0.172	1.099±0.182	-0.065	0.948
PrG_L_6_6	1.245±0.135	1.180±0.151	1.753	0.085
PrG_R_6_6	1.198±0.129	1.182±0.143	0.466	0.643

* indicates $P < 0.05$; HC, healthy control; CBF, cerebral blood flow; PrG, precentral gyrus; L, left; R, right.

3.4 Correlations Between ALFF, ReHo, CBF, and Clinical Scale Scores in Patients With Meige Syndrome

Pearson correlation analysis showed that, in patients with Meige syndrome, the ALFF value in the right medial superior frontal gyrus was negatively correlated with the mean Blepharospasm Disability Index score ($r = -0.452$, $P = 0.016$; Fig. 5A) and the total Blepharospasm Disability Index score ($r = -0.438$, $P = 0.020$; Fig. 5B). In addition, the ReHo value in the right medial superior frontal gyrus was negatively correlated with the Self-Rating Depression Scale score ($r = -0.385$, $P = 0.043$; Fig. 5C).

The normalized CBF value in PrG_L_6_2 was positively correlated with disease duration ($r = 0.429$, $P = 0.023$; Fig. 5D). However, no significant correlation was found between normalized CBF values in the precentral gyrus and dystonia severity scale scores in patients with Meige syndrome ($P > 0.05$).

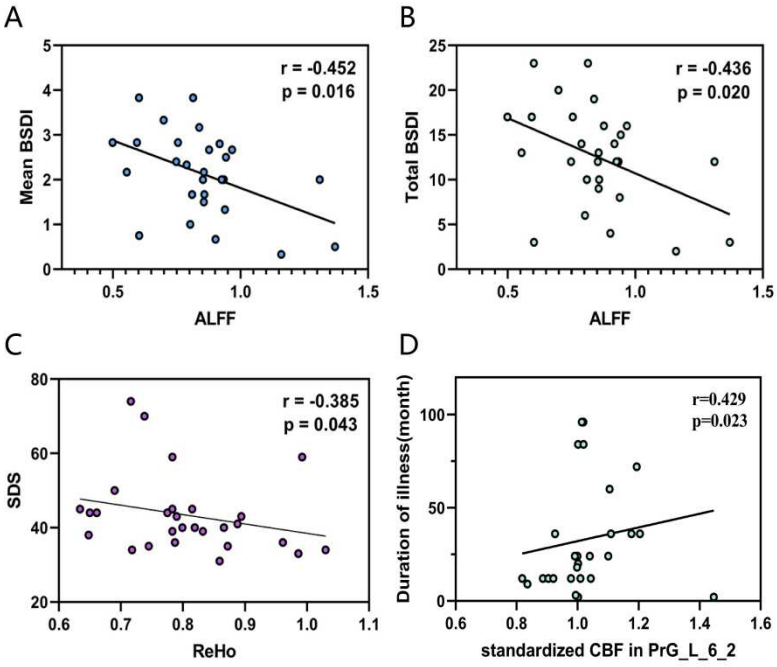


Fig. 5 Correlations between altered imaging metrics and clinical variables in patients with Meige syndrome.
Scatterplots show correlations between imaging metrics and clinical characteristics in patients with Meige syndrome. (A) ALFF values in the right medial superior frontal gyrus were negatively correlated with mean BSDI score (r = -0.452, P = .016). (B) ALFF values in the same region were negatively correlated with total BSDI score (r = -0.438, P = .020). (C) ReHo values in the right medial superior frontal gyrus were negatively correlated with SDS score (r = -0.385, P = .043). (D) Normalized CBF values in PrG_L_6_2 were positively correlated with disease duration (r = 0.429, P = .023).
Abbreviations: ALFF = amplitude of low-frequency fluctuation; ReHo = regional homogeneity; CBF = cerebral blood flow; BSDI = Blepharospasm Disability Index; SDS = Self-Rating Depression Scale; PrG = precentral gyrus; L = left.

3.5 ROC Curve Analysis

Receiver operating characteristic (ROC) curve analysis was performed using three parameters that showed significant between-group differences: the normalized CBF value in the right precentral gyrus, the ALFF value in the right medial superior frontal gyrus, and the ReHo value in the right medial superior frontal gyrus. The aim was to preliminarily evaluate their performance in discriminating Meige syndrome from healthy controls.

The area under the curve (AUC) for the normalized CBF value in the right precentral gyrus was 0.861, with a sensitivity of 60.7% and a specificity of 96.9%. The AUC for the ALFF value in the right medial superior frontal gyrus was 0.857, with a sensitivity of 89.3% and a specificity of 78.1%. The AUC for the ReHo value in the right medial superior frontal gyrus was 0.853, with a sensitivity of 67.9% and a specificity of 90.6% (Fig. 6).

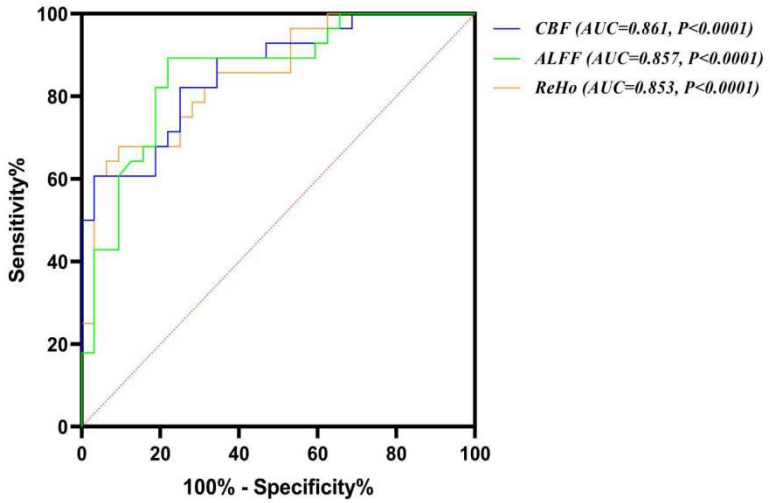


Fig. 6 Diagnostic performance of normalized CBF, ALFF, and ReHo for distinguishing patients with Meige syndrome from healthy controls.
Receiver operating characteristic curve analysis showed that normalized CBF in the right precentral gyrus, ALFF in the right medial superior frontal gyrus, and ReHo in the right medial superior frontal gyrus had good discriminative performance. The sensitivity, specificity, and AUC were 60.7%, 96.9%, and 0.861 for normalized CBF; 89.3%, 78.1%, and 0.857 for ALFF; and 67.9%, 90.6%, and 0.853 for ReHo, respectively.
Abbreviations: ROC = receiver operating characteristic; CBF = cerebral blood flow; ALFF = amplitude of low-frequency fluctuation; ReHo = regional homogeneity; AUC = area under the curve.

4. Discussion

By combining rs-fMRI and ASL, the present study compared differences in brain functional activity, as reflected by ALFF and ReHo, and cerebral perfusion in the primary motor cortex between patients with Meige syndrome and healthy controls. The results showed that patients with Meige syndrome exhibited abnormal brain functional activity and regional cerebral blood flow alterations, and that some imaging indices were associated with dystonia severity, emotional disturbances, and disease duration.

4.1 Altered Brain Functional Activity in the Medial Superior Frontal Gyrus

In the present study, patients with Meige syndrome showed decreased ALFF and ReHo values in the bilateral medial superior frontal gyri, as well as decreased ALFF in the left anteromedial cingulate gyrus. In addition, the ALFF value in the right medial superior frontal gyrus was negatively correlated with dystonia severity scores. These findings are generally consistent with previous studies [18]. The medial superior frontal gyrus is an important component of the supplementary motor area, which serves as a key node in the cortico-basal ganglia circuitry and is involved in voluntary movement, motor preparation, and the integration of complex motor sequences [19]. Therefore, reduced neural activity in

the medial superior frontal gyrus may indicate dysfunction of the supplementary motor area and may be related to impaired motor initiation, motor planning, and higher-order motor control in patients with Meige syndrome.

On the other hand, both the medial superior frontal gyrus and the left anteromedial cingulate gyrus are important nodes of the default mode network [20]. Previous studies have shown strong functional connectivity between the medial superior frontal gyrus and the anterior cingulate cortex [21], and abnormal activity in these regions has also been reported in Meige syndrome [18], suggesting that default mode network dysfunction may be involved in the abnormal motor control observed in this disorder. Meanwhile, the medial superior frontal gyrus is widely connected with key regions of the motor control network, including the precentral gyrus, caudate nucleus, and thalamus [22]. Taken together, decreased ALFF and ReHo values in the medial superior frontal gyrus may reflect local functional abnormalities within motor control-related networks and may be further associated with clinical manifestations of Meige syndrome, such as involuntary contractions of the eyelid and oromandibular muscles.

4.2 Correlations Between Functional Imaging Indices and Clinical Characteristics

The present study showed that the ALFF value in the right medial superior frontal gyrus was negatively correlated with both the mean and total Blepharospasm Disability Index scores in patients with Meige syndrome, suggesting that reduced ALFF in this region is associated with more severe blepharospasm-related disability and may serve as a quantitative imaging marker of symptom severity. This finding is broadly consistent with previous reports of medial frontal abnormalities in blepharospasm [23].

In addition, ReHo values in the bilateral medial superior frontal gyri were reduced, and the ReHo value in the right medial superior frontal gyrus was negatively correlated with the Self-Rating Depression Scale score. The medial superior frontal gyrus is located in the superior portion of the medial prefrontal cortex, a region that plays an important role in emotional regulation and is closely interconnected with limbic structures [24]. Abnormalities in this region have been widely implicated in the pathophysiology of psychiatric disorders such as depression [25]. Given that emotional disturbances are important nonmotor symptoms of primary dystonia [26], and that the depressive symptoms have been reported to be more common in patients with Meige syndrome than in healthy controls, the reduced ReHo in the medial superior frontal gyrus observed in this study may be related to nonmotor symptoms, including depression, in Meige syndrome. In the present cohort, 4 of 28 patients had depression, corresponding to a prevalence of 14.3%, which was markedly higher than the 12-month prevalence of major depressive disorder reported in Chinese adults (1.6%) [27]. On the other hand, no significant correlation was found between ReHo values in the medial superior frontal gyrus and dystonia severity scores, suggesting that altered local synchronization in this region may reflect a relatively stable disease-related functional characteristic rather than a direct marker of motor severity. Overall, abnormalities of the medial superior frontal gyrus may contribute to both motor and emotional disturbances in Meige syndrome and may represent a potential neuroimaging biomarker.

4.3 Altered Cerebral Perfusion in the Precentral Gyrus and Its Relationship With Clinical Characteristics

The present study found increased normalized CBF in the precentral gyrus in patients with Meige syndrome. As the primary motor cortex, the precentral gyrus is mainly involved in the preparation and execution of voluntary movement [28]. Dysfunction of this region may manifest as impaired motor inhibition, thereby leading to excessive muscle contraction, spasm, and abnormal involuntary movement [29]. Therefore, increased perfusion in the precentral gyrus may reflect an increased cortical load within the motor cortex during abnormal motor control in Meige syndrome.

Further analysis showed that the CBF value in PrG_L_6_2 was positively correlated with disease duration, suggesting that cerebral perfusion in the precentral gyrus may, to some extent, reflect disease progression. Previous studies have shown that symptomatic improvement in secondary dystonia is significantly associated with reduced regional CBF in the primary motor cortex, premotor cortex, supplementary motor area, and prefrontal cortex [30]. In addition, functional connectivity in sensorimotor-related brain regions has been reported to correlate significantly with symptom severity in patients with cervical dystonia [31]. Although these studies involved different dystonia subtypes, they all belong to the dystonia spectrum and collectively suggest that abnormalities in cerebral perfusion or brain functional activity within sensorimotor cortices may participate in disease progression and symptom expression, which is broadly consistent with the present findings.

4.4 Significance of the ROC Curve Analysis

As shown in Fig. 6, ROC curve analysis demonstrated that the normalized CBF value in the right precentral gyrus had a sensitivity of 60.7%, a specificity of 96.9%, and an AUC of 0.861. The ALFF value in the right medial superior frontal gyrus yielded a sensitivity of 89.3%, a specificity of 78.1%, and an AUC of 0.857. The ReHo value in the right medial superior frontal gyrus showed a sensitivity of 67.9%, a specificity of 90.6%, and an AUC of 0.853. Overall, all three imaging indices showed good discriminative performance, among which the normalized CBF value in the right precentral gyrus had the highest AUC and the highest specificity, suggesting that it may warrant further evaluation as an exploratory discriminative marker.

4.5 Limitations

This study has several limitations. First, the sample size was relatively small, and the findings require further validation in larger cohorts. Second, only single-post-labeling-delay ASL data were acquired in this study. Because relatively few time points were available for image registration within the sequence, the effectiveness of motion correction may have been limited, and residual motion-related artifacts may therefore have remained. Future studies using multi-post-labeling-delay ASL may improve the robustness of the findings. Third, because this was a cross-sectional study, causal relationships between the observed neuroimaging alterations and the development or progression of Meige syndrome cannot be established. Longitudinal studies, including assessments before and after treatment, are still needed to further clarify the underlying pathophysiological mechanisms.

5. Conclusion

Using rs-fMRI and ASL, the present study demonstrated reduced brain functional activity in the bilateral medial superior frontal gyri and the left anteromedial cingulate gyrus, together with increased cerebral perfusion in the precentral gyrus, in patients with Meige syndrome. These findings suggest that abnormal neural activity in the medial superior frontal gyrus may represent an important imaging feature of Meige syndrome and may be related to both motor and emotion-related abnormalities, whereas altered cerebral perfusion in the precentral gyrus provides new evidence for perfusion abnormalities in this disorder. Collectively, these results enrich current understanding of the neural mechanisms of Meige syndrome from the perspectives of both brain functional activity and cerebral blood flow, and the identified indices may serve as potential neuroimaging biomarkers. Further validation in larger samples and longitudinal follow-up studies is warranted.

Ethical statements

This study was approved by the Ethics Committee of China-Japan Friendship Hospital on September 13, 2022 (Approval No. 2022-KY-181). Written informed consent was obtained from all participants. All procedures were performed in accordance with the Declaration of Helsinki.

Data Availability Statement

The data that support the findings of this study are available from the corresponding author upon reasonable request.

Funding statement

This study was partly funded by the STI2030-Major Projects (No. 2022ZD0213300), the National Natural Science Foundation of China (No. 82271953 and U25A20136).

References

[1] LeDoux MS. Meige syndrome: what's in a name? Parkinsonism Relat Disord 2009;15:483–9. https://doi.org/10.1016/j.parkreldis.2009.04.006.

[2] Soland VL, Bhatia KP, Marsden CD. Sex prevalence of focal dystonias. J Neurol Neurosurg Psychiatry 1996;60:204–5. https://doi.org/10.1136/jnnp.60.2.204.

[3] Pandey S, Sharma S. Meige's syndrome: History, epidemiology, clinical features, pathogenesis and treatment. J Neurol Sci 2017;372:162–70. https://doi.org/10.1016/j.jns.2016.11.053.

[4] Liu J, Li L, Li Y, et al. Regional metabolic and network changes in Meige syndrome. Sci Rep 2021;11:15753. https://doi.org/10.1038/s41598-021-95333-8.

[5] Yao X-X, Li H-L, Wang S, et al. Brain functional network topology and connectivity in primary blepharospasm. Front Syst Neurosci 2025;19:1654795. https://doi.org/10.3389/fnsys.2025.1654795.

[6] Liu B, Mao Z, Yan X, et al. Structural network topologies are associated with deep brain stimulation outcomes in Meige syndrome. Neurother J Am Soc Exp Neurother 2024;21:e00367. https://doi.org/10.1016/j.neurot.2024.e00367.

[7] Jochim A, Li Y, Gora-Stahlberg G, et al. Altered functional connectivity in blepharospasm/orofacial dystonia. Brain Behav 2018;8:e00894. https://doi.org/10.1002/brb3.894.

[8] Yang A, Liu B, Lv K, et al. Altered coupling of resting-state cerebral blood flow and functional connectivity in Meige syndrome. Front Neurosci 2023;17:1152161. https://doi.org/10.3389/fnins.2023.1152161.

[9] Zang Y, Jiang T, Lu Y, et al. Regional homogeneity approach to fMRI data analysis. NeuroImage 2004;22:394–400. https://doi.org/10.1016/j.neuroimage.2003.12.030.

[10] Yang H, Long X-Y, Yang Y, et al. Amplitude of low frequency fluctuation within visual areas revealed by resting-state functional MRI. NeuroImage 2007;36:144–52. https://doi.org/10.1016/j.neuroimage.2007.01.054.

[11] Pakkenberg B, Bolwig TG, Pakkenberg H. Meige's syndrome: a neuropsychiatric disorder. Compr Psychiatry 1987;28:309–14. https://doi.org/10.1016/0010-440x(87)90066-6.

[12] Jankovic J, Kenney C, Grafe S, et al. Relationship between various clinical outcome assessments in patients with blepharospasm. Mov Disord Off J Mov Disord Soc 2009;24:407–13. https://doi.org/10.1002/mds.22368.

[13] Chao-Gan Y, Yu-Feng Z. DPARSF: A MATLAB Toolbox for "Pipeline" Data Analysis of Resting-State fMRI. Front Syst Neurosci 2010;4:13. https://doi.org/10.3389/fnsys.2010.00013.

[14] Yan C-G, Wang X-D, Zuo X-N, et al. DPABI: Data Processing & Analysis for (Resting-State) Brain Imaging. Neuroinformatics 2016;14:339–51. https://doi.org/10.1007/s12021-016-9299-4.

[15] Buxton RB, Frank LR, Wong EC, et al. A general kinetic model for quantitative perfusion imaging with arterial spin labeling. Magn Reson Med 1998;40:383–96. https://doi.org/10.1002/mrm.1910400308.

[16] Xu G, Rowley HA, Wu G, et al. Reliability and precision of pseudo-continuous arterial spin labeling perfusion MRI on 3.0 T and comparison with 15O-water PET in elderly subjects at risk for Alzheimer's disease. NMR Biomed 2010;23:286–93. https://doi.org/10.1002/nbm.1462.

[17] Fan L, Li H, Zhuo J, et al. The Human Brainnetome Atlas: A New Brain Atlas Based on Connectional Architecture. Cereb Cortex 2016;26:3508–26. https://doi.org/10.1093/cercor/bhw157.

[18] Wang Y, Luo M, Hou B, et al. Comparative study of brain activity and functional connectivity in

blepharospasm and blepharospasm-oromandibular dystonia. Front Neurol 2025;16:1583297. https://doi.org/10.3389/fneur.2025.1583297.

[19] Santosh CG, Rimmington JE, Best JJ. Functional magnetic resonance imaging at 1 T: motor cortex, supplementary motor area and visual cortex activation. Br J Radiol 1995;68:369–74. https://doi.org/10.1259/0007-1285-68-808-369.

[20] Franco AR, Pritchard A, Calhoun VD, et al. Interrater and intermethod reliability of default mode network selection. Hum Brain Mapp 2009;30:2293–303. https://doi.org/10.1002/hbm.20668.

[21] Li W, Qin W, Liu H, et al. Subregions of the human superior frontal gyrus and their connections. NeuroImage 2013;78:46–58. https://doi.org/10.1016/j.neuroimage.2013.04.011.

[22] du Boisgueheneuc F, Levy R, Volle E, et al. Functions of the left superior frontal gyrus in humans: a lesion study. Brain J Neurol 2006;129:3315–28. https://doi.org/10.1093/brain/awl244.

[23] Yang J, Luo C, Song W, et al. Altered regional spontaneous neuronal activity in blepharospasm: a resting state fMRI study. J Neurol 2013;260:2754–60. https://doi.org/10.1007/s00415-013-7042-8.

[24] Goodpaster CM, Christensen CR, Alturki M-B, et al. Prefrontal cortex development and its implications in mental illness. Neuropsychopharmacol Off Publ Am Coll Neuropsychopharmacol 2026;51:114–28. https://doi.org/10.1038/s41386-025-02154-8.

[25] Guo W, Cui X, Liu F, et al. Increased anterior default-mode network homogeneity in first-episode, drug-naive major depressive disorder: A replication study. J Affect Disord 2018;225:767–72. https://doi.org/10.1016/j.jad.2017.08.089.

[26] Stamelou M, Edwards MJ, Hallett M, et al. The non-motor syndrome of primary dystonia: clinical and pathophysiological implications. Brain J Neurol 2012;135:1668–81. https://doi.org/10.1093/brain/awr224.

[27] Zhao Y-J, Jin Y, Rao W-W, et al. Prevalence of Major Depressive Disorder Among Adults in China: A Systematic Review and Meta-Analysis. Front Psychiatry 2021;12:659470. https://doi.org/10.3389/fpsyt.2021.659470.

[28] Hanakawa T, Dimyan MA, Hallett M. Motor Planning, Imagery, and Execution in the Distributed Motor Network: A Time-Course Study with Functional MRI. Cereb Cortex N Y NY 2008;18:2775–88. https://doi.org/10.1093/cercor/bhn036.

[29] Delnooz CCS, Pasman JW, Beckmann CF, et al. Task-free functional MRI in cervical dystonia reveals multi-network changes that partially normalize with botulinum toxin. PloS One 2013;8:e62877. https://doi.org/10.1371/journal.pone.0062877.

[30] Kefalopoulou Z, Paschali A, Markaki E, et al. Regional cerebral blood flow changes induced by deep brain stimulation in secondary dystonia. Acta Neurochir (Wien) 2010;152:1007–14. https://doi.org/10.1007/s00701-010-0612-y.

[31] Feng L, Yin D, Wang X, et al. Brain connectivity abnormalities and treatment-induced restorations in patients with cervical dystonia. Eur J Neurol 2021;28:1537–47. https://doi.org/10.1111/ene.14695.